ELSEVIER

Journal of Power Sources 85 (2000) 245–253

JOURNAL OF POWER SOURCES

www.elsevier.com/locate/jpowsour

Capacity loss in Ni–Cd pocket plate batteries. The origin of the second voltage plateau

Elisabet Ahlberg [a,*], Ulrik Palmqvist [b], Nina Simic [a], Rune Sjövall [c]

[a] *Department of Chemistry, Göteborg University, SE-412 96 Göteborg, Sweden*
[b] *Arrhenius Laboratories, Stockholm university, SE-106 91 Stockholm, Sweden*
[c] *SAFT, Box 709, SE-572 28 Oskarshamn, Sweden*

Received 28 December 1998; received in revised form 22 June 1999; accepted 6 July 1999

Abstract

Electrical testing of batteries, voltammetry and surfaces analysis by X-ray diffraction (XRD) and Fourier transformation infrared (FTIR) were used to investigate the origin of the second voltage plateau. The electrical testing results show that there is a direct coupling between graphite loss and the appearance of the second voltage plateau. The graphite loss was shown to increase for float charging at elevated temperatures and high potentials. The effect of graphite particle size distribution was also investigated. Voltammetry of discharged material, $Ni(OH)_2$, and charged material, β-NiOOH and γ-NiOOH, in carbon paste showed that the second voltage plateau did not originate from the redox properties of the material, or the presence of carbonate in the material or in the electrolyte. Therefore, the second voltage plateau is believed to appear whenever an increased internal resistance arises, may it be due to graphite loss, swelling or some other factor.

Keywords: Capacity loss; Ni–Cd pocket plate batteries; Second voltage plateau

1. Introduction

The nickel–cadmium battery is an old and well investigated product very common in various kinds of applications, such as motor starts, uninterruptible power systems and emergency lighting. Despite long Ni–Cd experience, certain unexpected phenomena are now and then observed in pocket plate cells during operation. One such phenomenon is a second low voltage plateau in the discharge curve, predominantly occurring for cells in stationary applications. The appearance of the second plateau may be accompanied with a capacity loss. The origin of a second plateau in the discharge curve has been discussed since the beginning of this century and different explanations have been favoured during the years. In the early 1960s, it was believed to originate from the reduction of adsorbed oxygen, either on graphite present in the positive active material or on nickel hydroxide [1]. Later, Barnard et al. [2] proposed that the second plateau originated from an ohmic drop resulting from the formation of a barrier layer at the active material/electron collector interface. This view was further supported by the group of Zimmerman [3]. Recently, Sac-Epee et al. [4,5] showed that a direct transfer of γ-NiOOH to β-$Ni(OH)_2$ resulted in a low voltage plateau in the discharge curve. Furthermore, it was stated that the so formed β-$Ni(OH)_2$ was oxidised directly to γ-NiOOH, yielding a memory effect often observed in practice. [1] Despite these recent studies, a complete understanding of the phenomena has not been given.

The aim of the present investigation is therefore to contribute to the existing knowledge on this subject. In particular, we have investigated the electrochemical behaviour of positive active material from new and cycled batteries in carbon paste and compared these results with in-battery performance and phase composition; by X-ray diffraction (XRD), and Fourier transformation infrared (FTIR) spectroscopy. The batteries were chosen in such a

* Corresponding author. University of Göteborg, Department of Chemistry, SE-41296 Göteborg, Sweden. Tel.: +46-31-772-2879; fax: +46-31-772-2853; E-mail: ela@inoc.chalmers.se

[1] The term ''memory effect'' is normally used in relation to the negative electrode and partial cycling of the battery.

0378-7753/00/$ - see front matter
PII: S0378-7753(99)00340-7

way that comparison of some important processing parameters were possible. Thus, two different float charging potentials and two different temperatures were used to analyse the phase composition of the positive mass and the stability of graphite as a function of potential and temperature. The stability of graphite was also investigated with regard to its size distributions. Material from a new battery (no float charging) was used as a reference. The results show that high potential, elevated temperatures and small graphite particles contribute to the origin of a second voltage plateau in the discharge curve.

1.1. Charge / discharge reactions

In Scheme 1, the overall reactions and phase transformations occurring during charge and discharge of the positive electrode are shown [6–8]:

During charge β-$Ni(OH)_2$ is transformed into β-NiOOH with a 15% decrease by volume. Further charging promotes the formation of γ-NiOOH. The formation of the γ-phase is accelerated by high charging rate, elevated temperature and high electrolyte concentration. The volume increase is 44% compared to β-NiOOH. Discharging of γ-NiOOH occurs normally via an intermediate phase, α-$Ni(OH)_2$. This transformation is accompanied with another 39% volume increase [8]. Recently, a new route was proposed involving a direct and reversible transfer of γ-NiOOH to β-$Ni(OH)_2$ [4,5]. All these transformations, and the β-NiOOH to γ-NiOOH transformation in particular, show that the charge/discharge involves drastic volume changes. These changes, or swelling, will of course affect the electrode pocket and the strip of the pocket in some sense. It has been stated that the appearance of a second plateau in the discharge curve is always related to a poor electronic active material and that the width of the plateau is proportional to the amount of the γ-phase. Poor electronic conduction in the positive active mass will give a non-uniform current distribution and as a consequence, γ-NiOOH can be formed directly from β-$Ni(OH)_2$ [4]. For a positive pocket electrode, which contains graphite, poor electronic conduction can be obtained if large amounts of the graphite are oxidised. According to Singh [8], swelling introduces microcracks during charge/discharge resulting in an increased surface area of the electrode active material. Impeding the overcharging can significantly reduce the swelling.

1.2. The second voltage plateau

The shape of the second voltage plateau has been shown to vary from a simple change of the slope to a significant step resulting in a plateau with 200–300 mV lower potential. Since the capacity of the battery is given at a specific potential, the occurrence of the second plateau is normally connected with a capacity loss. Discharge at various rates has, however, a clear effect on the appearance of the second plateau. At high rates (large discharge currents) the plateau is more pronounced. This is an indication of an enhanced internal resistance in the positive electrode material [1–3]. The hypothesis is that swelling, due to structural changes of the unit cell volume between charged NiOOH and discharged $Ni(OH)_2$, impairs the contact between nickel active material and the graphite during successive charges/discharges and causes a second plateau in the discharge curve.

1.3. The effect of carbonate

It has been stated that the decrease of electrode capacity becomes more severe at high discharge rates and at high carbonate concentrations [9]. This degradation depends primarily on the positive active material, but at higher carbonate levels also on the negative material [1]. The discharge curves exhibit a plateau located about 180 mV below that of a standard curve. As the carbonate concentration in the electrolyte increases the hydroxide concentration decreases and a lowering in the electrolyte conductivity is expected. This will result in a larger ohmic drop and cause a change in potential. However, impedance measurements of active material in electrolytes with varying degree of carbonation show that the increase in electrolyte resistance is too small to account for a 180 mV shift in potential [9].

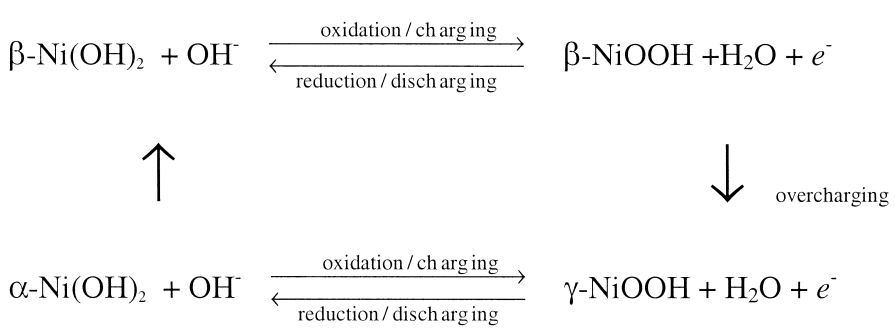

Scheme 1. Bode's diagram.

1.4. Graphite oxidation

The origin of carbonate in the electrolyte is mainly from the oxidation of graphite. In alkaline solutions graphite is oxidised and covered with an oxide film. In addition to this, CO, CO_2 and O_2 is also formed at high anodic potentials [10]. The surface oxide formed has a quinone-type structure and can be reduced. The oxidation reactions of graphite are given in Scheme 2.

For example, elevated temperature and high charging potentials accelerate the graphite oxidation. The rate of reaction is proportional to the number of active groups on the surface. It has been shown for other applications that the orientation of the graphite particles is decisive for its reactivity, and flakes with large area to edge ratio is less reactive. The reason for this is that the active groups are only present at the edges, where the structure has open bonds.

As can be seen in Scheme 2 the formation of carbonate diminishes the concentration of hydroxide ions in solution; for each mole of carbonate formed 6 mol of hydroxide ions are consumed. A lower hydroxide concentration will actually favour the reduction (discharging) of NiOOH, Scheme 1. As the reduction proceeds hydroxide ions are formed and the reaction rate diminishes. This will result in a sloping discharge curve.

1.5. Effects of cobalt additions

To avoid swelling, cobalt is commonly used as an additive in commercial nickel electrodes. The cobalt addition is believed to increase the conductivity of the active material and to facilitate the charging (oxidation) of nickel hydroxide [11].

In Fig. 1, it can be seen that at the potential range of the nickel electrode, cobalt exists as trivalent CoOOH. Trivalent co-precipitated cobalt in the $Ni(OH)_2$ matrix increases the chargeability of the nickel hydroxide. This has been explained by improved conductivity in the discharged state [12] and/or by increased amount of proton vacancies [13]. They suggest that the proton vacancies shift the oxidation potential less anodic and thereby the chargeability and electrochemical efficiency will be improved. In another study [11], bivalent $Co(OH)_2$ was added to the nickel

$$C + 2OH^- \rightarrow CO_{ads} + H_2O + 2e^-$$
$$CO_{ads} + 2OH^- \rightarrow CO_{2,ads} + H_2O + 2e^-$$
$$CO_{ads} \rightarrow CO(g)$$
$$2CO_{ads} \rightarrow O_2(aq) + 2C$$
$$CO_{2,ads} \rightarrow O_2(aq) + C$$
$$CO_{2,ads} \rightarrow CO_2(g)$$
$$CO_2(g) + 2OH^- \rightarrow CO_3^{2-} + H_2O$$

Scheme 2. Oxidation of graphite.

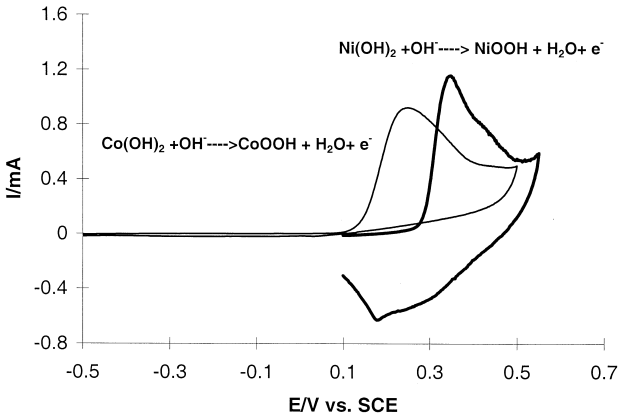

Fig. 1. A comparison of the voltammetric behaviour of $Co(OH)_2$ and $Ni(OH)_2$ in carbon paste. Sweep rate 1 mV s^{-1} and electrolyte concentration 1 M KOH.

active material. During charging of the electrode, the cobalt hydroxide was oxidised to trivalent CoOOH. The presence of CoOOH was claimed to change the potential barrier of the intercalation process in the γ-NiOOH formation, and thereby the formation of γ-NiOOH is hindered. A defective structure of γ-NiOOH is anyhow formed with a charge acceptance, i.e. electrons emitted, higher than 3 per molecular unit (the value typical for β-NiOOH). During the reduction of the defect γ-NiOOH, CoOOH fragments act as nuclei for the crystallisation of the β-$Ni(OH)_2$, and assist in increasing the depth of discharge.

2. Experimental

2.1. Electrode definitions

The main composition of the positive electrode active material in the investigated pocket plate battery cells (denoted [A]–[E] below) was β-$Ni(OH)_2$ and graphite. One electrode [E] also contained small amounts of cobalt. The number of electrodes tested in each group ranged from two to four.

Type [A]: Reference cell without float charging;
Type [B]: Float charged at 1.42 V at room temperature during 2 years;
Type [C]: Float charged at 1.8 V at room temperature during 2 years;
Type [D]: Float charged at 1.42 V at 40°C during 3 years;
Type [E]: Float charged at 1.42 V at 40°C during 3 years.

2.2. Electrical testing of the batteries

The capacity measurements were performed at a discharge rate of $0.2C_5$ A and $1.0C_5$ A to a specific voltage. Charging was performed at $0.2C_5$ A. The electrode potential was monitored vs. a Zn/ZnO reference electrode during the electrical measurements. In all cases the studied cells showed a positive limitation. Prior to testing, the cells were subjected to a formation procedure in order to activate the materials. In one case, a [C] electrode was analysed after float charging without the formation procedure.

After the electrical testing, the electrode active material used for the analyses was dismantled followed by thorough washing and drying. The active material was washed with deionized water until the pH was in the range 9–10 of the ''outlet water''. In the case of charged material, drying in vacuum at room temperature or 60°C immediately followed dismantling.

2.3. Electrochemical experiments

For the more fundamental experiments, a conventional three-electrode cell was used with platinum gauze as the auxiliary electrode. The potential was measured against a saturated potassium chloride calomel electrode, $E = 241.5$ mV with respect to SHE. The cell used was made of polypropylene. All experiments were carried out at room temperature. The electrolyte was purged with highly purified nitrogen for at least 30 min before the experiment was started. A nitrogen gas flow was maintained above the solution during the experiment, to prevent oxygen contamination. An EG&G Princeton Applied Research Potentiostat/Galvanostat Model 273A were used.

Besides the electrode active materials from the dismantled cells, also technical quality $Ni(OH)_2$ and $Ni_3CO_3(OH)_4 \cdot 4H_2O$ (Ni-hydroxy-carbonate) were tested. The Ni-hydroxy-carbonate was from Merck; extra pure.

2.3.1. Electrolyte preparation

The pure electrolytes used during the voltammetric measurements were either electrolyte consisting of 5.2 M KOH with addition of LiOH, or 3.5 M KOH without additions. The potassium carbonate concentration in these electrolytes was below 3 g l^{-1}. In order to simulate high carbonate levels, CO_2(g) was bubbled into the electrolyte until the desired CO_3^{2-} concentration, given as K_2CO_3, was obtained. This electrolyte consisted of 103 g l^{-1} K_2CO_3, 3.5 M KOH and LiOH. In some cases, an electrolyte with higher carbonate concentration was used; 190 g l^{-1} K_2CO_3, 2.1 M KOH and LiOH.

2.3.2. Preparation of the carbon paste electrode

The carbon paste electroactive electrode (CPEE) can be used to study low conducting substances and consists of commercial carbon paste with a non-conducting binder (Metrohm) and finely grained samples. The carbon paste and the sample were thoroughly mixed together in a mortar in order to obtain a homogeneous paste. The electroactive paste was placed as an approximately 1.5 mm thick layer over a carbon paste layer, which had been previously filled and pressed into an epoxy cavity. This was done in order to ensure adhesion between the electroactive paste and the rest of the electrical connections in the electrode. The surface of the electrode was smoothened with a spatula and excess paste was removed with a sharp steel blade. Electrical connection to the graphite paste was made with a platinum wire at the bottom of the cavity. The platinum wire was plugged into a brass rod. The geometrical area of the electrode surface was 0.2 cm^2. The mixing ratios (by weight) used were E:CP (Electroactive material:Carbon Paste) = 1:3 for the reference material [A], 1:6 for the [D] and [E] material, and 1:12 for Ni-hydroxy-carbonate. The E:CP ratios were optimised for physical stability and current response. The carbon paste electrode technique has recently been used in fundamental studies of the negative electrode [14,15].

2.4. Chemical and surface analyses

2.4.1. Chemical analyses

Carbonate and hydroxide concentrations were measured by ordinary acid–base titration. The amount of graphite present in the positive electrodes was obtained as the residue after dissolution and filtering of active material in strong hydrochloric acid.

2.4.2. Sieving

The graphite particle size distribution was determined with sieves providing fractions below 71 μm, fractions in the range 71 to 315 μm, and fractions exceeding 315 μm.

2.4.3. XRD

Phase composition was determined by XRD using a powder diffractometer SIEMENS D5000. During the powder analysis, the diffractometer was equipped with a position sensitive detector (PSD) and the radiation source used was CuK_α. The CuK_β-radiation was absorbed in a Ni filter. The measurements were made at 0.02° intervals of 2θ over the range 10–75° using a cumulated count-time of 10 s for each step.

2.4.4. FTIR spectroscopy

All samples were analysed by transmission FTIR spectroscopy, using the standard KBr disk technique. The IR-spectra were obtained using a Perkin-Elmer 1800 Fourier Transform Infrared Spectrometer equipped with a DTGS detector.

3. Results and discussion

3.1. Electrical testing

It is known that an unused cell does not exhibit any second voltage plateau, neither at high carbonate concen-

Table 1
Electrolyte composition, graphite loss and swelling of the positive active material

Tested electrode material	K_2CO_3 concentration ($g\ l^{-1}$)	Degree of carbonation (%)	Electrolyte density ($g\ cm^{-3}$)	Graphite loss (wt.%)[a]	Swelling (%)
[A]	12	4.0	1.20	undetectable	39
[B]	31	13	1.16	undetectable	30
[C]	$153/97_1/75_2/23_3$	$72/32_1/24_2/7.0_3$	$1.16/1.20_1/1.21_2/1.20_3$	8	24
[D]	$138/31_1/6.0_2/3.0_3$	$46/9.0_1/2.0_2/1.0_3$	$1.22/1.21_1/1.21_2/1.21_3$	33	44
[E]	–	–	–	–	–

[a]Calculated with reference to the initial graphite content.
The subscripts 1, 2 and 3 used in columns 2–4 denotes the value obtained after the 1st, 2nd and 3rd electrolyte exchange.

tration and/or at high discharge rates. However, after float charging at constant potential the second voltage plateau can be observed.

In Table 1, the different materials are listed together with the electrolyte composition, the degree of carbonation, graphite loss and swelling. For the electrodes [C] and [D] a number of electrolyte exchanges were made during the laboratory experiments and the corresponding changes are also given in the table. The subscripts 1, 2 and 3 denotes the value obtained after the 1st, 2nd and 3rd electrolyte exchange.

In Fig. 2, the discharge curves for the [C] and [D] electrodes (discharged at $0.2C_5$ A) are shown together with the discharge curve for the reference electrode. The discharge curve for the [B] electrode; float charged at 1.42 V at room temperature, resembles the discharge curve of the reference electrode. The second voltage plateau (300 mV for [D]) result in a capacity loss that seems to be related to the graphite loss in the material (Table 1). The capacity to a specific voltage degrades as the effect of the second plateau increases (Figs. 2 and 3). The second plateau effect becomes more accentuated at $1.0C_5$ A compared to $0.2C_5$ A for the [D] electrode, indicating a resistance problem. At $1.0C_5$ A, only about 20% of the active material is used, as measured to the end voltage of 1.5 V vs. Zn/ZnO. This should be compared with about 40% at $0.2C_5$ A.

For the [C] electrode the carbonation is very high and the density low, as shown in Table 1, i.e., the electrolyte resistance cannot be neglected for the applied discharging currents. Therefore, the initial potential level for the [C] electrode is somewhat lower compared with the [D] electrode (Figs. 2 and 3). The electrolyte resistance is likely higher in the pores of the active materials compared to the bulk solution. In particular, this should be prevailed for the positive active material during overcharging since OH^- is consumed during the formation of NiOOH, and since graphite oxidation consumes OH^- as well. This results in low concentrations of OH^- and relatively high concentrations of CO_3^{2-} in the pores of the positive active material. The low densities observed ($1.16\ g\ l^{-1}$) are due to the handling of the cells during the electrical testing, i.e., the filling up with water, etc. Despite the elevated electrolyte resistance, the second voltage plateau cannot be observed for the [C] electrode (Fig. 2). The absence of the second plateau is likely due to the low graphite loss. Despite low graphite loss in the [C] electrode, compared to [D], the concentration of K_2CO_3 in the electrolyte is high. A

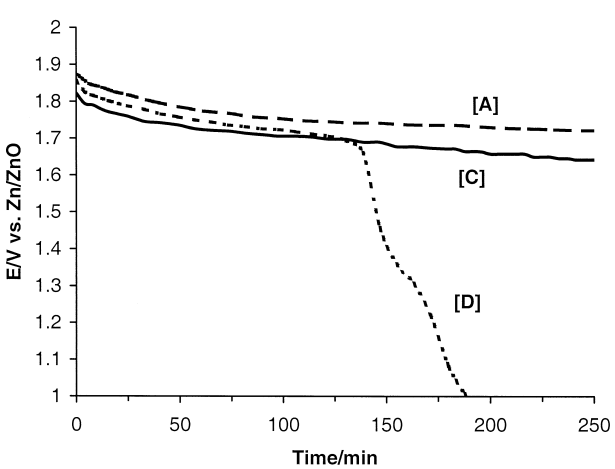

Fig. 2. Discharge curves, $0.2C_5$ A, showing a second voltage plateau for the positive electrode [D]. [C] has been subjected to float charging during 2 years at room temperature, and [D] to float charging during 3 years at 40°C. For comparison, the discharge curve for the reference [A] is also shown. [A] has not been subjected to float charging.

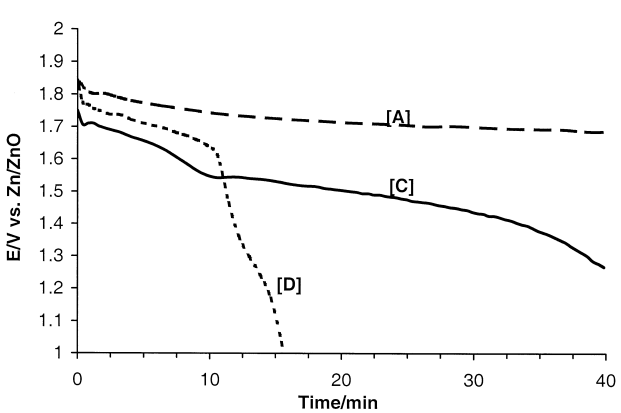

Fig. 3. Discharge curves, $1.0C_5$ A, showing a second voltage plateau for the positive electrode [D]. [C] has been subjected to float charging during 2 years at room temperature, and [D] to float charging during 3 years at 40°C. For comparison, the discharge curve for the reference [A] is also shown. [A] has not been subjected to float charging.

simple calculation shows that the graphite loss (1.9 g) on this positive electrode gives a K_2CO_3 concentration of about 160 g l^{-1}. The value observed was 153 g l^{-1}, Table 1, indicating a good agreement with the calculated value. Hence, the graphite loss in the [C] electrode is due to the oxidation of graphite. For the [D] electrode the graphite loss (33%) is much higher than the corresponding carbonate concentration in the electrolyte which leads to the conclusion that a large part of the graphite has fallen down and settled at the bottom of the cell. This conclusion is also supported by the fact that the swelling of the [D] electrode (44%) is higher compared to the [C] electrode (24%), since the swelling can promote the graphite to fall down to the bottom of the cell. Another important difference between the [D] and [C] electrodes is that [D] has been subjected to several capacity determinations by discharge cycles while the [C] electrode has been on continues constant current charging. For the same reason, no second plateau is observed for the [C] electrode at $1.0C_5$ A (Fig. 3). The slight dip observed after about 10 min, is not a second plateau, but rather an effect of an abrupt potential shift in the negative electrode (instrumental effect).

After electrolyte exchanges in the cell with the [C] electrode, the positive curve is just parallel shifted about 150 mV to more positive potentials (Fig. 4). This is probably due to the lower electrolyte resistance obtained. For the [D] electrode, the discharge curves still show a second voltage plateau after electrolyte exchanges (Fig. 5). This further indicates that there is a permanent effect due to the material itself rather than to the electrolyte. Furthermore, no parallel shift is observed, since the density is unchanged.

A comparison between reference positive material, [A], and [D] and [E] ([E] is known to not exhibit a second voltage plateau), shows that the graphite from the [A] and [D] electrodes exhibit a totally different distribution of the particle size compared with the [E] electrode (Fig. 6). The graphite in the former electrodes contains a large amount

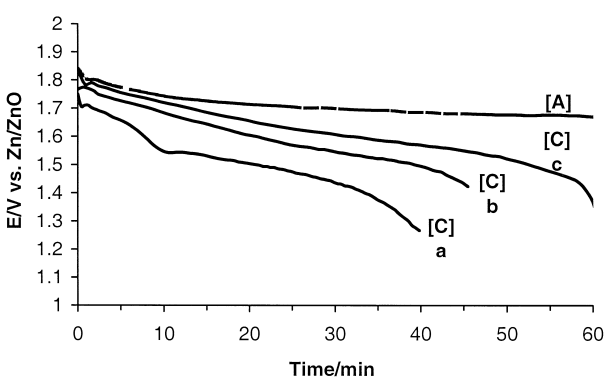

Fig. 4. Discharge curves, $1.0C_5$ A, for the [C] electrode, subjected to float charging during 2 years at room temperature, (a) without electrolyte exchange, (b) after one electrolyte exchange and (c) after three electrolyte exchanges. For comparison, the discharge curve for the reference [A] is also shown.

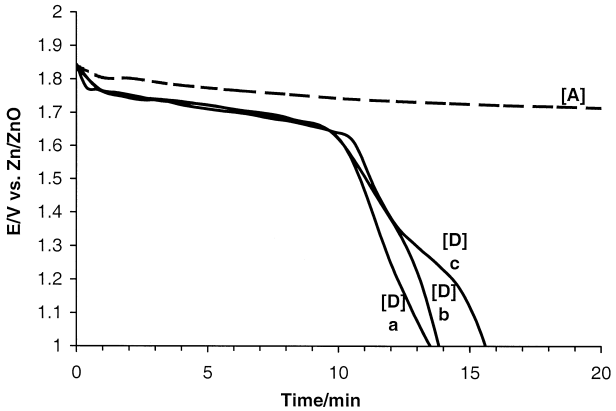

Fig. 5. Discharge curves, $1.0C_5$ A, for the [D] electrode, subjected to float charging during 3 years at 40°C, (a) without electrolyte exchange, (b) after one electrolyte exchange and (c) after three electrolyte exchanges. For comparison, the discharge curve for the reference [A] is also shown.

of a small fraction. Therefore, the carbonation probably is considerably higher in these electrodes compared to the [E] electrode (Section 1.4).

Swelling is a phenomenon that may affect the performance of the cell during charge/discharge cycling and float charging. Since the pocket is attached to the side beading, the swelling is higher in the middle of the pocket compared to the end.

For the reference cell [A] the swelling is about 40% and similar values are obtained for the float charged [B], [C] and [D] electrodes (for [E] no value of the swelling is available). This indicates that the observed difference in capacity and appearance of a second voltage plateau cannot be explained by the swelling effect alone. However, swelling in combination with graphite loss will further increase the internal resistance in the electrode, due to an increased porosity leading to the deterioration of electrical conductivity.

3.2. Voltammetry

Cyclic voltammetry on CPEE was made to investigate the redox properties of positive active material from different Ni–Cd batteries. For comparison, the voltammetric behaviour of technically pure $Ni(OH)_2$ and a Ni-hydroxycarbonate ($NiCO_3 \cdot 2Ni(OH)_2$), was also investigated. These measurements aimed to separate out the electrochemical properties from other effects that might be involved in the generation of a second voltage plateau in the discharge curves.

For technically pure $Ni(OH)_2$ the results resembled those in the reference electrode used, [A]. The influence of different parameters on the voltammetric response was tested; sweep rate, switching potential and hold time at the most positive potential. In Fig. 7 the sweep rate dependence for the reference material is shown. The anodic peak shifts in the positive direction as the sweep rate increases,

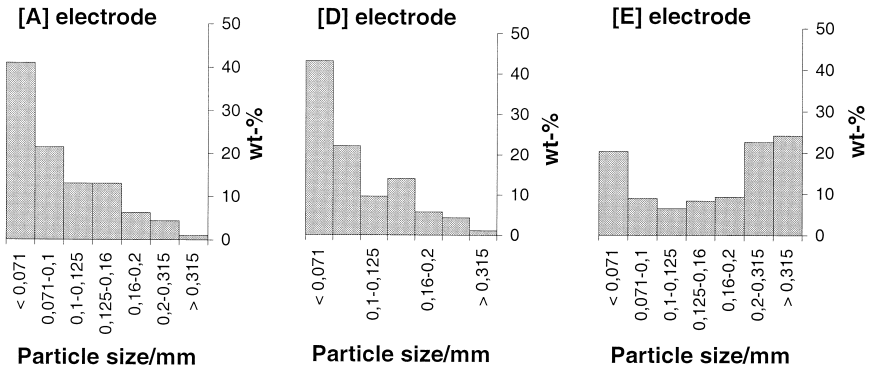

Fig. 6. Particle size distribution of graphite in the electrodes.

while the cathodic peak position is largely uninfluenced by changes in the sweep rate. This indicates that the oxidation process involves slow electron transfer kinetics while the reduction process is more reversible. As the sweep rate increases the reduction wave becomes broader, which probably reflects the incorporation of hydroxide ions and the corresponding electrolyte cation in the $Ni(OH)_2$ formed from NiOOH (Scheme 1). The charge ratio between the anodic and cathodic processes, Qa/Qc, is close to 1 for the sweep rates used in this investigation. This indicates that the total reaction is reversible.

$$Ni(OH)_2 + OH^- \Leftrightarrow NiOOH + H_2O + e^- \quad (1)$$

Different switching potentials were tested and it can be concluded that the voltammetric behaviour is the same irrespective of the positive potential limit. Also for different hold times at the most positive potential, the voltammetric response remains the same.

The different materials tested exhibit similar voltammetric behaviour with some exceptions (Fig. 8). The Ni-hydroxy-carbonate exhibits two anodic waves, one for the oxidation of Ni(II) bound to hydroxide ions, which appear at the same potential as for pure $Ni(OH)_2$, and one for the oxidation of Ni(II) bound to carbonate. The oxidation of the carbonate bound nickel seems to be slightly facilitated. This, however, does not influence the reduction process, which appears at the same potential as for the reference electrode material [A]. For the [D] electrode, the voltammogram is broad, indicating slower kinetics or higher internal resistance in these masses compared to the reference material. It should be noted that the actual masses are mixed with conducting carbon paste and one would expect that the resistance in the electrode is negligible.

The voltammetric data were evaluated with respect to peak potentials and peak currents. The peak current was directly proportional to the sweep rate as expected for a solid state reaction. The peak potential was found to be a function of the logarithm of the sweep rate. The potential for the reduction process is largely independent of sweep rate for all materials. For the oxidation process, the peak

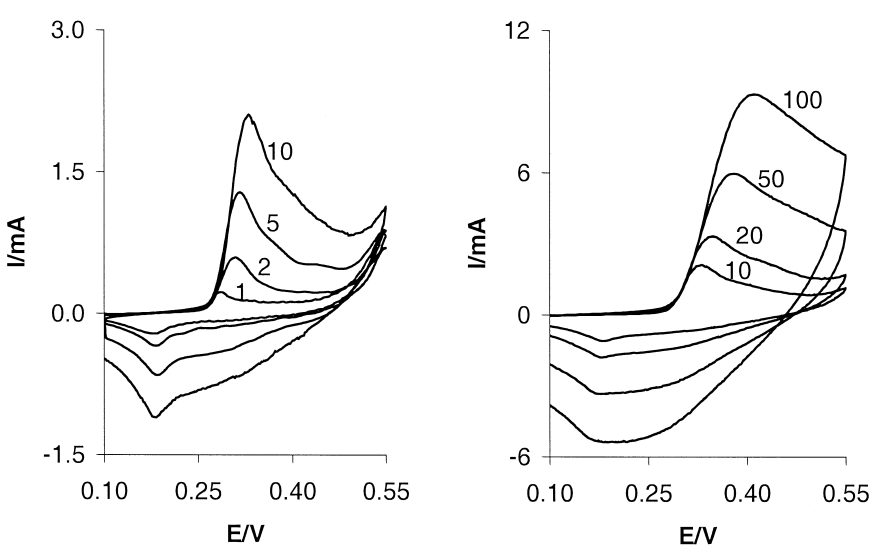

Fig. 7. Sweep rate dependence on the voltammetric behaviour of [A] in carbon paste; E:CP = 1:3. Battery electrolyte containing 103 g l^{-1} carbonate. The numbers denote the sweep rate in mV s^{-1}.

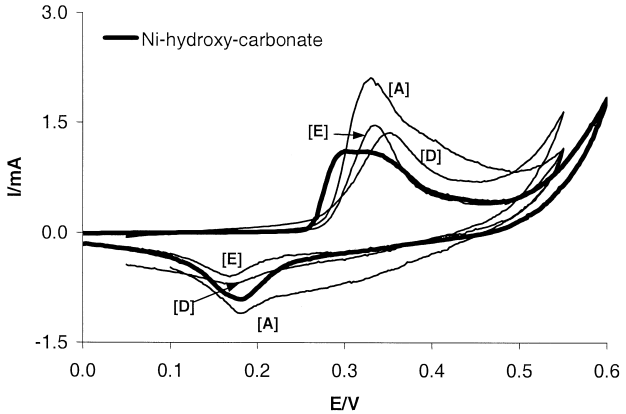

Fig. 8. Cyclic voltammetry for positive materials in carbon paste; E:CP = 1:3 for [A], 1:6 for [D] and [E], and 1:12 for Ni-hydroxy-carbonate. Battery electrolyte containing 103 g l^{-1} carbonate. Sweep rate 10 mV s^{-1}.

potential increases linearly with the logarithm of the sweep rate and two different phenomena are observed. For the reference material [A] a shift of about 60 mV $decade^{-1}$ is observed, while for [D] and [E] the peak potential changes with 30 mV $decade^{-1}$. This difference in reaction kinetics does, however, not seem to influence the charging/discharging properties.

To further investigate the redox behaviour of discharged positive material and correlate that to battery performance, the material was oxidised in a battery electrolyte containing 190 g l^{-1} K_2CO_3, 2.1 M KOH and significant amounts of LiOH. A constant charging potential was applied for 100 s and then a discharging measurement was made at constant applied current (0.1 mA) (Fig. 9). The reference material [A] and the [D] material exhibit similar behaviour with two plateaus in the discharge curve, corresponding to the $Ni(OH)_2$/NiOOH and $Ni(OH)_2$/Ni redox couples, respectively. For [E] an additional plateau is observed, probably due to hydrogen evolution. There is a potential

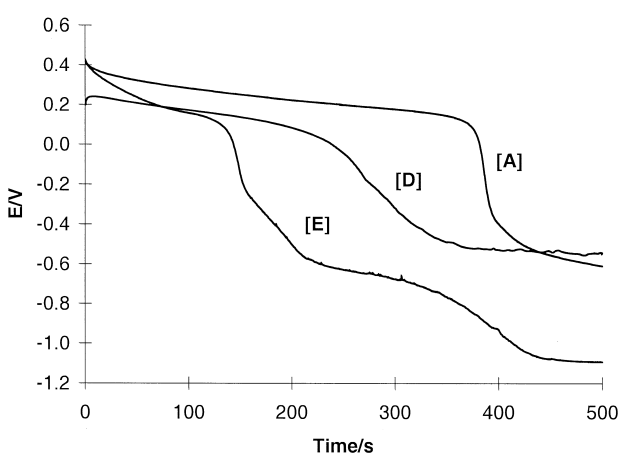

Fig. 9. Constant current potentiometry of slightly oxidised (500 s at 1.6 V) positive material. $I = -0.1$ mA. Battery electrolyte containing 103 g l^{-1} carbonate.

difference between the reference material [A] and the battery masses of about 100 mV, and the transition from one plateau to the next is also more drawn out. This indicates that the battery masses have higher resistance and slower reaction kinetics. In Fig. 9, it is only the appearance of the curves that is important, and not the discharge time, because the amount of material in the carbon paste differs.

Voltammetric measurements were also made on charged material with start at the open circuit potential. The voltammetric result was the same as for oxidised uncharged material, irrespective of the composition of the charged material, i.e., β-NiOOH and/or γ-NiOOH.

In conclusion, the voltammetric results in combination with XRD and FTIR measurements (Section 3.3), show that the capacity loss or the appearance of a second voltage plateau in the discharge curve are not due to the redox properties of the material, or to the presence of carbonate in the material or in the electrolyte. It seems that the capacity loss is accentuated in the 3-dimensional pore structure found in the pocket plates under certain circumstances and can therefore be regarded as a resistance problem.

3.3. Surface analysis

The XRD analysis of the different positive active materials is presented in Table 2. The gamma phase was found in the charged electrodes [C] and [D]. The [C] electrode contained the largest amount of the γ-phase. The reason for this is probably that this electrode was taken directly from float charging, without any pre-electrical testing, before the XRD measurement. The charged reference [A] has not been float charged and consequently did not contain any γ-NiOOH. The same observation was made for the charged [B] electrode. This electrode was, however, cycled before the XRD, and the obtained diffractogram was almost identical with that of β-$Ni(OH)_2$. The state of charge was confirmed by electrochemical experiments. This special charged phase is formed during prolonged

Table 2
XRD results of the positive active materials

Electrode material	β-$Ni(OH)_2$	β-NiOOH	γ-NiOOH
[A] discharged	X	d.l.	–
[A] charged	x	X	–
[B] charged	–	X*	–
[C] charged	d.l.	x	X
[D] discharged	X	x	–
[D] charged	X	x	X
[E] discharged	X	x	–
$Ni(OH)_2$ technical quality	X	–	–

X = Significant amounts.
x = Detectable amounts.
d.l. = At the detection limit.
X* = Charged material showing the same diffraction pattern as β-$Ni(OH)_2$.

charging at controlled relatively low potentials at room temperature. The existence of this phase makes it impossible to determine the state of charge only by examining the sample with XRD. Further works are in progress for crystal structure determination of the new phase.

Scanning tunnelling microscopy was recently used to trace the conformational changes of the surface film formed on nickel in alkaline solution [16]. It was stated that as the nickel hydroxide was oxidised, the structure was largely unaltered until the formation of γ-NiOOH took place at higher potentials. This further support the existence of a charged phase with a structure resembling that of β-$Ni(OH)_2$.

The positive active material from batteries with high carbonate electrolyte concentration showed trace amounts (at the noise level) of carbonates. The X-ray measurements indicated, however, that the carbonate was some type of nickel carbonate rather than crystallised electrolyte, like K_2CO_3 or Li_2CO_3.

The FTIR analyses confirmed the results from XRD and no further substances could be detected, indicating that crystalline products are formed. $Ni_3CO_3(OH)_4$, that has been suggested as a candidate for the origin of the second voltage plateau, could not be observed in the FTIR analyses.

4. Conclusions

The main conclusions of this investigation are summarised below.

There is a direct coupling between the graphite loss and the extent of the second voltage plateau. This is interpreted as a result of increased internal resistance in the electrode.

- At elevated temperatures, the graphite loss is accelerated, resulting in increased internal resistance and high carbonate concentrations in the electrolyte.
- A combination of a high graphite loss and swelling increase the extent of the second voltage plateau, due to increased internal resistance.
- The graphite loss seems to be favoured by a large fraction of small graphite particles.

After long-time float charging at room temperature, no capacity loss or second voltage plateau was observed, irrespective of charging potential. However, at elevated temperatures a second voltage plateau is observed.

Voltammetric measurements in combination with XRD and FTIR analyses show that the second voltage plateau is not due to the redox properties of the material, i.e., γ-NiOOH or β-NiOOH, or the presence of carbonate in the material or in the electrolyte.

Acknowledgements

We would like thank MSc H. Malm, Mr. T. Tran, Mr. E. Andersen and MSc U. Thuresson for their contribution to this study.

References

[1] S.U. Falk, J. Electrochem. Soc. 107 (1960) 661.
[2] R. Barnard, G.T. Crickmore, J.A. Lee, F.L. Tye, J. Appl. Electrochem. 10 (1980) 61.
[3] A.H. Zimmerman, in: D.A. Corrigan, A.H. Zimmerman (Eds.), PV 90-4, The Electrochemical Society, Pennington, 1990, p. 311.
[4] N. Sac-Epee, M.R. Palacin, B. Beaudoin, A. Delahaye-Vidal, T. Jamin, Y. Chabre, J.-M. Tarascon, J. Electrochem. Soc. 144 (1997) 3896.
[5] N. Sac-Epee, M.R. Palacin, A. Delahaye-Vidal, Y. Chabre, J.-M. Tarascon, J. Electrochem. Soc. 145 (1998) 1434.
[6] H. Bode, K. Dehmelt, T. Witte, Electrochim. Acta 11 (1966) 1079.
[7] R. Barnard, C.F. Randell, F.L. Tye, J. Appl. Electrochem. 10 (1980) 127.
[8] D.J. Singh, J. Electrochem. Soc. 145 (1998) 116.
[9] D.L. Barney, A.J. Catotti, S.F. Pensabene, J. Power Sources 3 (1971) 119.
[10] T. Arikado, C. Iwakura, H. Yoneyama, H. Tamura, Electrochim. Acta 21 (1971) 551.
[11] O.G. Malandin, B.B. Ezhov, Russ. J. Electrochem. 31 (1995) 368.
[12] A. Audemer, A. Delahaye, R. Farhi, N. Sac-Epee, J.-M. Tarascon, J. Electrochem. Soc. 144 (1997) 2614.
[13] M.C. Bernard, M. Cortes, H. Keddam, P. Takenouti, P. Bernard, S.J. Senyarich, Power Sources 63 (1996) 247.
[14] N. Simic, E. Ahlberg, J. Electroanal. Chem. 451 (1998) 237.
[15] N. Simic, E. Ahlberg, J. Electroanal. Chem. 462 (1999) 34.
[16] S.-L. Yau, F.-R. Fan, F.T.P. Moffat, A.J. Bard, J. Phys. Chem. 98 (1994) 5493.